Progress in Nuclear Energy 105 (2018) 124–135

Contents lists available at ScienceDirect

Progress in Nuclear Energy

journal homepage: www.elsevier.com/locate/pnucene

The path for innovative severe accident neutronics studies in ZPRs. Part II.2 - Interpretation of SNEAK-12B experiment for core disruption in LMFBRs impact of nuclear data uncertainties on reactivity coefficients

M. Margulis[a,b,*], P. Blaise[a], F. Mellier[a], E. Gilad[b,**]

[a] DEN/CAD/DER/SPESI/LP2E, CEA Cadarache, Saint-Paul-lez-Durance 13108, France
[b] The Unit of Nuclear Engineering, Ben-Gurion University of the Negev, Beer-Sheva 84105, Israel

ARTICLE INFO

Keywords:
SNEAK-12B
Core disruption
Severe accidents
LMFBR
Sensitivity analysis
Uncertainty analysis

ABSTRACT

The present work details further information regarding a new benchmark to be introduced to the international community, for dealing with neutronic code validation in the frame of the analysis of severe accidents in fast reactors leading to core degradation and material relocation. This specific benchmark is based on further analysis of selected experiments performed at the Schnelle Null-Energie-Anordnung Karlsruhe (SNEAK). The SNEAK-12B core was loaded with plutonium fuel to better represent future fast systems and the experiments considered fuel relocation and redistribution of structural material. In this paper, the experimental results are analyzed by state of the art tools, Serpent-2 Monte Carlo and the ERANOS code for deterministic calculations. The paper presents a full sensitivity and uncertainty analysis based on the JEFF-3.1.1 and the associated covariance data COMAC-V01, which is performed in order to gain deeper insight into the governing phenomena related to geometrical changes of the core. A comparison of the propagated uncertainties between Serpent and ERANOS is made. The uncertainty propagation vary from code to code, and strongly disagree in most cases of axial fuel relocation. This is evident for small reactivity variation (< 1 cent), where the difference in the propagated uncertainties obtained from the two codes is vividly visible. The analysis provide valuable information on uncertainty propagation in a system where the overall material balance is not modified, and contributes to the design of future experiments. This work is done within the frame of new core design capacities and innovative experimental programs to be implemented in Zero Power Reactors, such as the ZEPHYR project led independently by CEA.

1. Introduction

The selected advanced nuclear energy systems under the Generation IV program provide some significant advances over current-generation nuclear energy systems in the areas of sustainability, economics, safety and reliability, proliferation resistance, and finally in physical protection. The six selected systems employ a large spectrum of fuels, a variety of core geometries, and various coolants. These systems introduce modeling challenges that differ from current-generation Light Water Reactors (SCAs). Therefore, while mature tools and data exist for analyzing LWR under normal and under severe core accident (SCA) conditions, the ability of these tools to model accurately the advanced systems, under different conditions, has to be assessed systematically.

Predictions of advanced systems operations are of limited accuracy due to the uncertainties inherent to the nuclear data for a variety of important nuclides relevant to reactor design. The uncertainties of those nuclides strongly affect the design margins required to ensure safe operation and introduce large discrepancies to calculations of the core behavior under stressed conditions (SCA) (Rullhusen, 2005; Salvatores et al., 2008).

The uncertainties are associated with both design and nuclear data propagated uncertainties. Design uncertainties are associated with the design margins and their respect to core geometry, materials, and the assessed working parameters. Nuclear data uncertainties gather the uncertainties the impeded in nuclear data measurements (reaction rates, detector efficiency, etc.). Significant uncertainties exist in the data for minor actinides, as well as for some of the more common fissionable materials (in certain energy ranges), and in non-fuel materials such as Bismuth and Lead in particular. Furthermore, uncertainties result from the different available nuclear data (ENDF, JEFF, etc.),

* Corresponding author. The Unit of Nuclear Engineering, Ben-Gurion University of the Negev, Beer-Sheva 84105, Israel.
** Corresponding author.
E-mail addresses: marat.margulis@cea.fr, maratm@post.bgu.ac.il (M. Margulis), gilade@bgu.ac.il (E. Gilad).

https://doi.org/10.1016/j.pnucene.2018.01.002
Received 16 July 2017; Received in revised form 19 December 2017; Accepted 11 January 2018
Available online 30 January 2018
0149-1970/

where large discrepancies could be found, e.g., Sodium (Tommasi et al., 2010; Margulis et al., 2017a).

Ideally, the uncertainties should be provided in a form of covariance matrices from the production process of nuclear data libraries. To obtain reliable covariances associated with the JEFF-3.1.1 evaluations (Salvatores et al., 2008), the nuclear data for major isotopes was re-evaluated with a series of targeted experiments. The result of this work led to the generation of a new set of covariance matrices linked to the JEFF-3.1.1 nuclear data, i.e., the COvariance MAtrices Cadarache (COMAC) (De Saint Jean et al., 2012). The COMAC provides a solution to an important need of covariance data for sensitivity and uncertainty analysis.

The SNEAK-12B experimental program was carried out during the 80 s at the Karlsruhe center (KfK). The aim of the experimental program was to study effects of large fuel relocation by simulating SCA environment in a plutonium-loaded core. The experimental program included axial fuel slump-out and slump-in of different sizes, radial fuel slump-out and a single experiment for fuel slump in. In addition, streaming channels blockage was simulated by placing steel blockage at different axial locations in the central core assemblies. The results from the SNAEK-12B core were utilized for code validation of Monte Carlo codes, i.e., Serpent 2 MCNPX, and the deterministic code ERANOS (Margulis et al., 2017b).

This paper presents a further investigation of the SNEAK-12B core, focusing on the sensitivity and uncertainties studies to evaluate the impact of neutron cross-section uncertainty on the core reactivity. This study is part of a larger scientific project aiming at studying the possibility of recriticality in a fast reactor due to material relocation, where the parameter of interest is the reactivity changes between different states of SCA progression (Margulis et al., 2017c, 2017a, 2017b). These studies provide new insights and shed light on the validity of the neutron cross-section generated for fast spectrum reactors and potentially indicate the isotopes for which the cross-section data needs to be improved.

The analysis of the SNEAK–12B core is carried out as a part of a larger study focused on recriticality possibilities in Fast Breeder Reactors (FBR) as part of a scientific collaboration program between CEA Cadarche (France) and Ben-Gurion University of the Negev (Israel) for future experimental program design that would be implemented in Zero power Experimental PHYsics Reactor (ZEPHYR) (Blaise et al., 2016), which aims to study neutronic aspect of SCA in FBR.

1.1. The ZEPHYR project

Post Fukushima review of reactor regulation in France, lead to the closure of two zero-power facilities at the CEA site in Cadarache by the end of 2018. The future critical facility ZEPHYR, to be critical by 2025, is an investment to be made by CEA to replace EOLE and MINERVE facilities for the next 5 decades. For the last decades, the MINERVE ZPR has produced a large range of experimental data, mainly for LWRs but also for the fast spectrum reactors through the PHENIX and the SUPERPHENIX projects (Blaise et al., 2016). In parallel with R&D studies about sodium fast reactor (Ohshima et al., 2016), in particular the ASTRID (Bertrand et al., 2016; Gabrielli et al., 2015) industrial demonstrator, a new interest for fast-thermal coupled cores has risen up (Ros et al., 2017; Aufiero et al., 2016). Those configuration consist of getting fast-spectrum neutronics characteristics in reduced central zone, also called the “experimental zone”, while criticality is achieved thanks to a thermal driver zone, in which the majority of fission reactions are gathered. such configurations allow an important reduction of the fissile materials and higher flexibility due to the thermal spectrum kinetic parameters. The main issue is then to provide a proper fast spectrum in the center, which achieved by the correct adaptation of the conversion zone, which surrounded by the thermal spectrum zone. Hence, with the new awaited innovative feature of the ZEPHYR project, coupled core physics is one of the most promising outcomes for performing neutron physics and improve both codes and nuclear data.

One particular advantage of the fast/thermal ZEPHYR configuration is the improvement of spectrum and reativity effects representativity in the fast zone against infinite lattice fast cells. This advantage is currently under investigation for experimental studies of representative severe accident scenarios accusing in full power sodium-cooled fast reactors, to be loaded into the core of a ZPR, with the main focus on the representativity of the reactivity variations (Ivanov et al., 2013; Margulis et al., 2017d, 2017e). The revision of the SNEAK-12A (Margulis et al., 2017a) and SNEAK-12B was made in order to study the behavior of a fast system under different SCA configuration, in terms of reactivity variation sensitivity. This revision would shed light on the behavior of the sensitivity/uncertainty of modification in material, geometry or both, and provide indication for the future experiment design.

2. SNEAK-12B - Experimetal facility overview

An extensive program for experimental studies related to fast reactors was carried out at the Kernforschungzentrum Karlsruhe (KfK), currently Forschungszentrum Karlsruhe (FZK), over a period of 20 years (60's-80's). The main research was carried out at the SNEAK facility. This effort was carried out in support of the German fast reactor program, that led to the construction of the KNK-II facility. This section provides a short overview of the SNEAK–12B core geometry outlines, loaded with plutonium-oxide-uranium-oxide fuel rods. The fuel was selected according to the desire to examine the behavior of plutonium fuel under SCA conditions. The fuel cell geometry had to be designed in such way that compression of fuel would be possible. The core specification of the SNEAK–12B geometry, material balance and experimental procedures are summarized in the safety reports of the reactor available through the International Reactor Physics Experiment Evaluation (IRPhE) project of the OECD Nuclear Energy Agency (Margulis et al., 2017b; Frohlich et al., 1980; Ivanov and Duranti, 2006).

2.1. Core description

The SNEAK-12B consists of mixed types fuel configurations, i.e., plate and rod, and is cooled by air, which flows through the gaps between the fuel assemblies. The total core area including unused areas (filled with air) is 326.4×326.4 cm^2 and a total height of about 260 cm. The active cores area is 130.56×130.56 cm^2 with about 82 cm in height surrounded by 30 cm of upper and lower reflectors, which make a total height of about 140 cm. The core consists of four main radial zones: the radial blanket (same as in SNEAK-12A (Margulis et al., 2017c)), the driver zone, the buffer region, and the central core and test zone, as shown in Fig. 1. The core reactivity is controlled by 16 shim rods (marked by blue and red squares in Fig. 1a) located at the driver zone region.

All the assemblies radial cross-section make 5.44×5.44 cm^2. The driver and blanked zones assemblies are filled with horizontal plates type fuel, an example of the driver zone assembly shown in Fig. 2. The buffer and the center core fuel assemblies containe a varied number of rod lattices from 13 to 39 rods per lattice. The rods are 0.67 cm in diameter with 0.07 cm clad thickness. Representative fuel elements for normal loading of central core fuel assembly is shown in Fig. 3, where the active core region (marked in purple in Fig. 3a) loaded with seven equal length MOX rodlets (marked in purple Fig. 3), for which the radial distribution is shown in Fig. 3b. The blanket and axial reflector are composed of depleted uranium dioxide (marked in orange, Fig. 3). The full specification of the SNEAK-12B core is presented in (Margulis et al., 2017b).

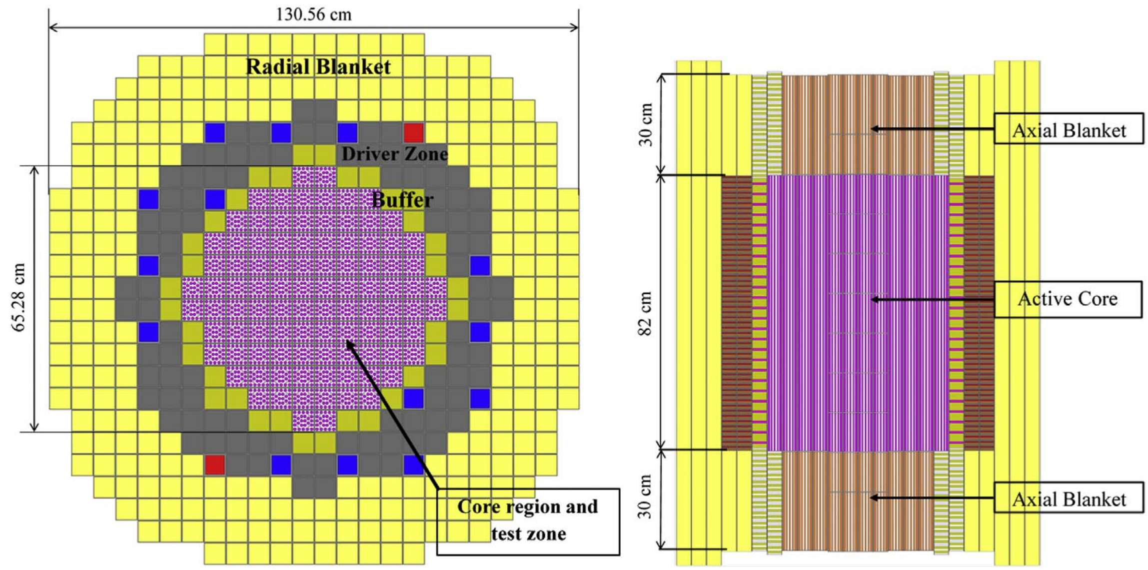

(a) XY cross section. **(b)** XZ cross section.

Fig. 1. SNEAK-12B core layout and dimensions. The blue and red squares indicate on the shim rod positions. (For interpretation of the references to colour in this figure legend, the reader is referred to the Web version of this article.)

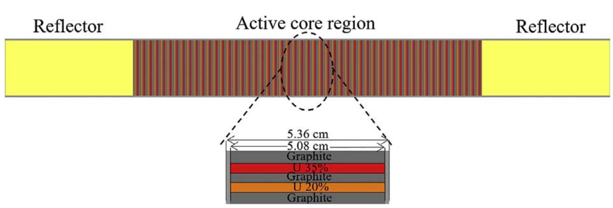

Fig. 2. Representative SNEAK-12B driver zone fuel assembly.

2.2. Experimental configurations

During the experiments the number of rods per bundle was changed in the center region of the test zone. In the most compacted loading the number of rods in the lattice reached 39 fuel rods, as shown in Fig. 4. By removing rods, it could be reduced to any number below 26 (Fig. 3b). The bundle frame was stabilized by four steel support rods. In order to

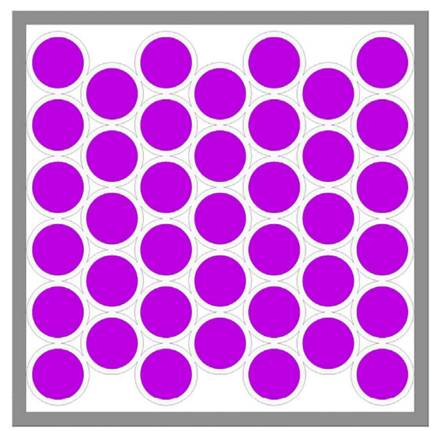

Fig. 4. SNEAK-12B 39 fuel rod compacted configuration.

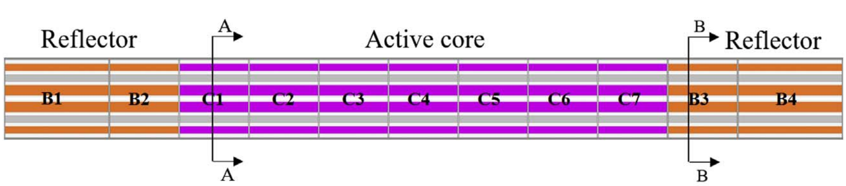

(a) Representative fuel assembly.

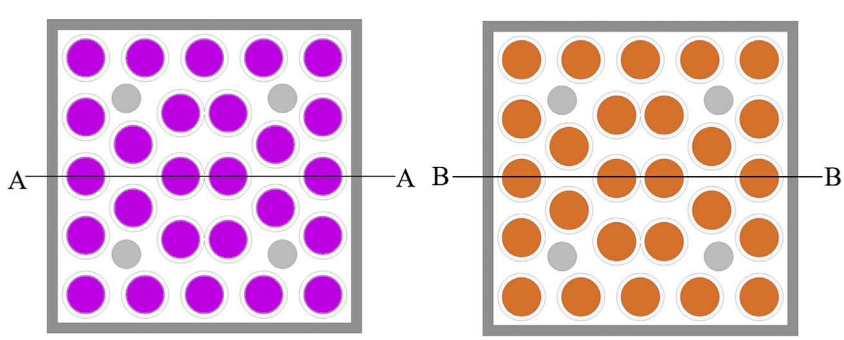

(b) Plutonium rod arrangement. **(c)** Reflector rod arrangement.

Fig. 3. XZ and XY plane cross sections of a representative center core fuel assembly.

Table 1
Axial experiment loading for SNEAK-12B center core.

Experiment	Modified elements	Description of loading (number of rodlets in the sections).											ID
		B1	B2	C1	C2	C3	C4	C5	C6	C7	B3	B4	
Slump-out	4	x	x	x	x	39	0	39	x	x	x	x	1
	16												2
	4	x	x	39	x	x	0	x	x	39	x	x	3
	16												4
	4	x	x	x	x	x	0	x	x	39	39	x	5
	16												6
Slump-in	4	x	x	x	x	19.5	39	19.5	x	x	x	x	7
	16												8
	4	x	x	19.5	x	x	39	x	x	19.5	x	x	9
	16												10
	4	x	x	0	x	x	39	39	x	x	x	x	11
	16												12
Slump-through	4	x	x	13	x	x	x	x	x	39	x	x	13
	16												14
	16	x	x	13	13	x	x	x	39	39	x	x	15
Steel insertion	4	x	x	SS	x	x	x	x	x	SS	x	x	16
	4	x	x	x	x	x	x	x	x	SS	SS	x	17
	12	x	x	x	x	x	SS	x	x	x	x	x	18
	12	x	x	x	x	x	x	x	x	SS	x	x	19
Large vertical move	12	x	x	x	x	0	0	39	39	39	39	x	20
	12	x	39	39	39	0	0	0	39	39	39	x	21
	12	x	x	0	0	39	39	39	39	x	x	x	22
	12	x	39	0	0	0	39	39	39	39	39	x	23

allow a vertical variation of the fuel density, the loading of the central 16 elements was subdivided into 7 core bundles, about 11 cm in length each (C1 to C7) and 2 axial blanket regions, which are composed of 2 bundles each (B1 and B2 correspond to the bottom reflector and B3 and B4 correspond to the upper reflector), as shown in Fig. 4.

In this paper, four types of SNEAK-12B experiments are analyzed:

- Fuel worth experiments - The number of rods per bundle or element was changes in the central 1 or 4 elements.
- Axial fuel redistribution experiments - The number of rods per element was decreased in one axial section and increased correspondingly in another one (in 4 or 16 elements).
- Radial fuel redistribution experiments - Fuel was displaced radially by decreasing the number of rods per element in some elements and correspondingly increasing it in the neighboring elements. The size of the modified zone varied between 12 and 48 elements.
- Steel redistribution experiments - Stainless steel was loaded into the void space between the rods of the normal bundles in 1 or 2 axial section of 4 or 12 elements.

Details of those experiments are given in Table 1 (the table headers correspond to the different regions in the center core assembly as shown in Fig. 3) for axial and in Fig. 5 for redial fuel movements. The 19.5 fuel rods per region presented in Table 1 is a notation for an average amount of fuel rods (e.g., for 4 affected bundles there are two bundles with 20 fuel rods and two bundles with 19, making an average of 19.5 fuel rods per bundle). In Fig. 5 the letter stands for blanket (B), driver zone (D), buffer (F) and shim rod (S), whereas the blank (white) squares correspond to unchanged fuel bundles. The reactivity effects were measured by compensation using shim rod calibration in the SNEAK core. From the replicability when measurements were repeated the accuracy is estimated to be about 0.2 cents.

3. Methodology

As mentioned above, a further analysis of the SNEAK-12B was carried out in order to study the effect of the cross-section data on future experiments design. The calculations were carried out mainly with the JEFF-3.1.1 cross-section libraries. For all experimental configuration, the impact of nuclear data uncertainty for several isotopes is studied (^{6}C, ^{16}O, ^{27}Al, ^{56}Fe, ^{58}Ni, ^{234}U, ^{235}U ^{238}U, ^{238}Pu, ^{239}Pu, ^{240}Pu, ^{241}Pu, ^{242}Pu and ^{241}Am). These isotopes have the largest impact on the results. Each isotope information (cross-section, differential data, covariances) is processed in 33 energy groups for the perturbation method. In the experiments from the SNEAK-12 program (SNAEK-12A), an evaluation of the nuclear data libraries was made (Margulis et al., 2017a), with the main focus on a specific isotope, i.e., ^{23}Na. The sodium isotopes experience large differences between the JEFF-3.1.1 and the ENDF-VII.0/1 nuclear data libraries. In the case of the SNEAK-12B campaign sodium was not present in large quantities (only in the shim rods), thus intuitively it was excluded from the calculations. In this work, such comparison was excluded since none of the major isotopes mention above experience such large difference between the two libraries (JEFF and ENDF).

In the present work, two codes are utilized in order to estimate the sensitivity profiles of each experimental configuration, i.e., Serpent 2 and ERANOS. Serpent 2 is a continues-energy Monte Carlo reactor physics code (Leppanen et al., 2015). In recent years Serpent 2 was equipped with collision history method for evaluating the sensitivity coefficients for both reaction rates ratios and ratios of bilinear functions (Aufiero Maand Bidaud et al., 2015). ERANOS (Ruggieri et al., 1973) is a reactor analysis code system that has been extensively used for fast reactor physics and analysis. In particular sensitivity and uncertainty analysis of a given reactor configuration. In this paper additional comparison between Serpent and ERANOS is made on the SNEAK-12B experimental configurations.

4. Sensitivity and uncertainty analysis results

4.1. Clear (unperturbed) reference core

The sensitivity profiles shed some light on the governing reactivity mechanisms, e.g., the dominant response types and the energy range in which they exhibit maximal impact that influences particles' transport in a particular experiment. Furthermore, analyzing the experimental and calculated results along with the sensitivity between different experiments could substantially increase the amount of information which can be deduced from experiments, rather than just comparing

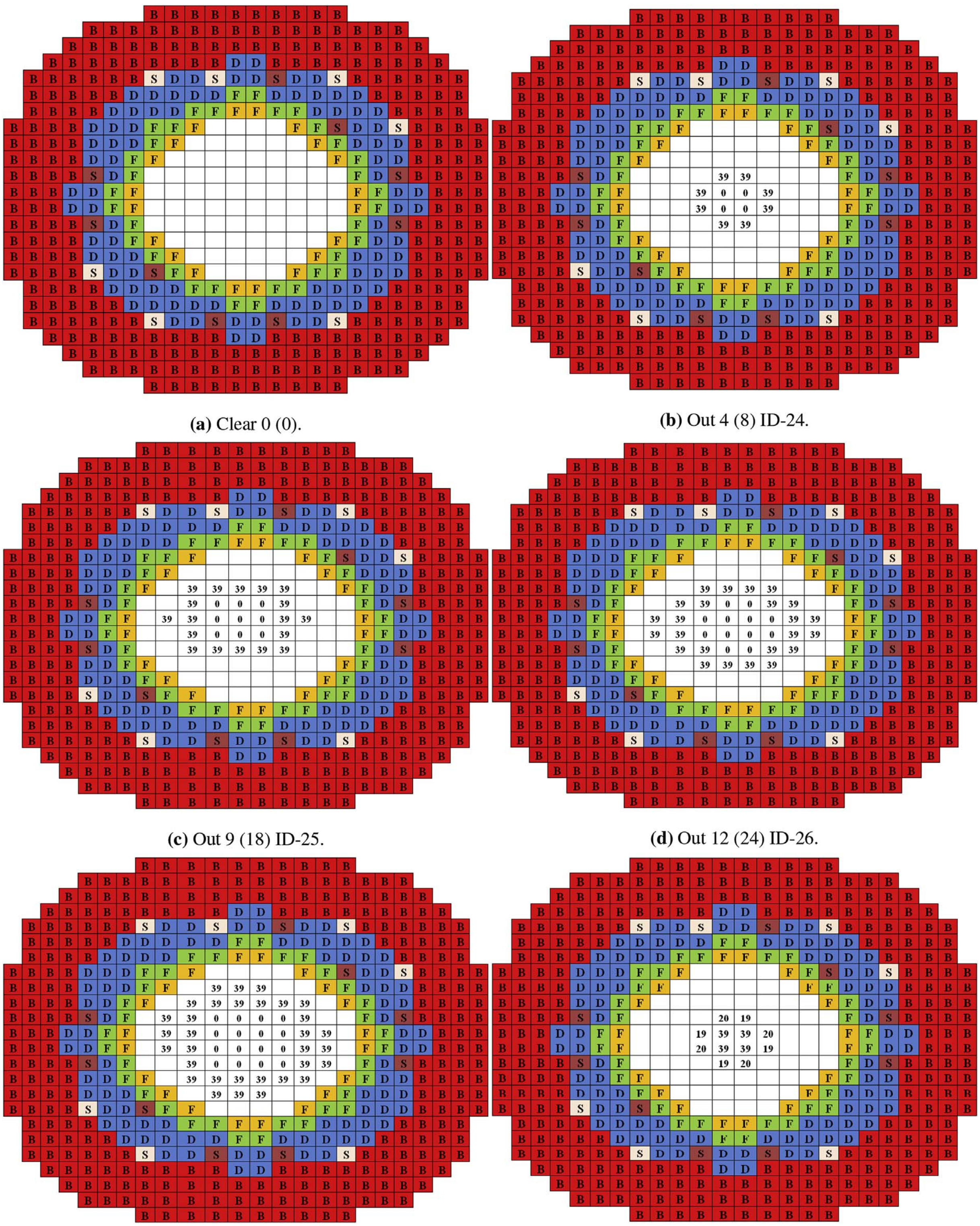

(a) Clear 0 (0).

(b) Out 4 (8) ID-24.

(c) Out 9 (18) ID-25.

(d) Out 12 (24) ID-26.

(e) Out 16 (32) ID-27.

(f) In 4 (8) ID-28.

Fig. 5. Outwards and inwards core configurations for SNEAK-12B experiments (Blanket (B), Driver, (D), Buffer (F), Shim rod (S), and blank is unperturbed).

the values.

The cross-section sensitivity analysis of the SNEAK-12B core is initially carried out on the clear (unperturbed) core configuration in order to determine the capabilities of the two codes (Serpent and ERANOS) and evaluate the discrepancies between them if present. An example for the k_{eff} sensitivity to several response types of selected nuclides (e.g., ^{239}Pu, ^{240}Pu, ^{235}U, and ^{238}U) is shown in Figs. 6–9. For the shown isotopes there is no large difference between the two codes. All the isotopes are summarized in Tables 2 and 3. The results are in a good agreement for the most sensitive isotopes such as uranium and plutonium. Sensitivity coefficients with values less than or equal to 1.00E-03 are with small significance due to low concentration in the system. However, one isotope stands out; the carbon isotope exhibits large difference between the two calculations. The graphic representation of

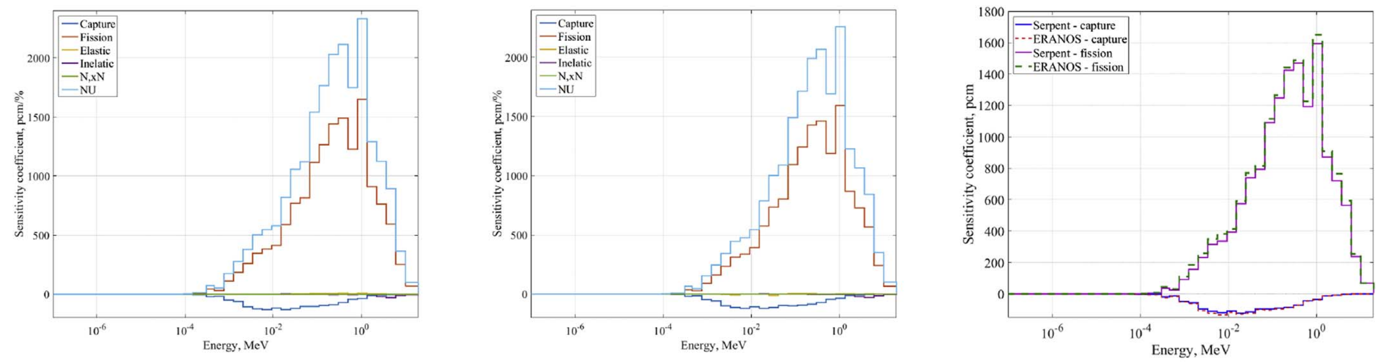

(a) ERANOS. **(b)** Serpent. **(c)** ERANOS-Serpent comparison.

Fig. 6. Clear criticality core multiplication factor sensitivity to ^{239}Pu cross-sections.

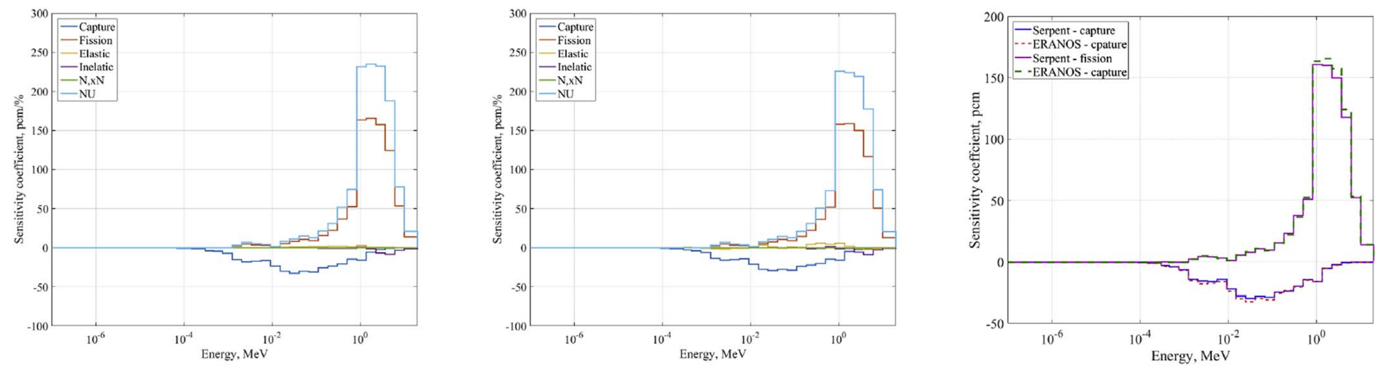

(a) ERANOS. **(b)** Serpent. **(c)** ERANOS-Serpent comparison.

Fig. 7. Clear criticality core multiplication factor sensitivity to ^{240}Pu cross-sections.

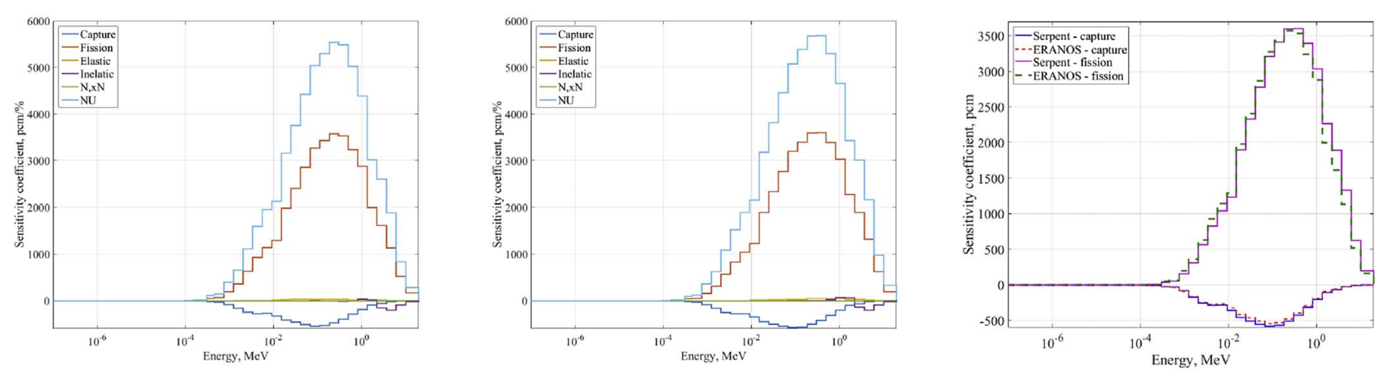

(a) ERANOS. **(b)** Serpent. **(c)** ERANOS-Serpent comparison.

Fig. 8. Clear criticality core multiplication factor sensitivity to ^{235}U cross-sections.

the carbon sensitivity profiles is given in Fig. 10. The large difference could be attributed to the small changes that were required in the R-Z model in ERANOS.

In order to evaluate the uncertainties associated with the cross-section data, the clear core configuration sensitivity profiles need to be assessed through a multigroup cross-section variance and covariance process. This is done by utilizing the data available in the COMAC covariance matrix. The corresponding uncertainties to each of the response functions are shown in Fig. 11, the total uncertainties are summarized in Table 4, and the propagated uncertainties per isotope are summarized in Tables 5 and 6.

The results in Fig. 11 show that the highest propagated uncertainties are in the capture and fission reactions of ^{235}U and ^{238}U, which is similar to the uncertainties associated with the SENAK-12A experiments (Margulis et al., 2017a). The high level of uncertainties is not very surprising in the uranium isotope, due to large uncertainties in the high neutron energy range in the covariance data, as shown in Figs. 12 and 13. The third high contribution to the uncertainties is associated with the plutonium-239 isotope. The covariance matrix and the uncertainty vectors are shown in Fig. 14. The uncertainties in the covariance data are not large (in comparison to uranium isotopes). Therefore, the relatively high uncertainty is a result of the high plutonium density in the center and buffer zones. It should be noted that all isotopes show high uncertainties in the high neutron energy range. The flux spectrum of the

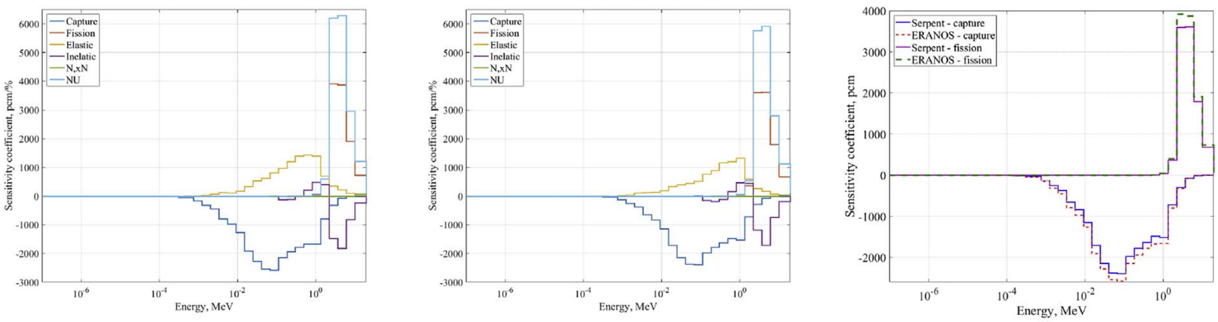

(a) ERANOS. **(b)** Serpent. **(c)** ERANOS-Serpent comparison.

Fig. 9. Clear criticality core multiplication factor sensitivity to ^{238}U cross-sections.

Table 2
Total sensitivity coefficients calculated by ERANOS for R-Z model with JEFF-3.1.1 - Clean core [pcm/%].

Nuclide	Capture	Fission	Elastic	Inelastic	N,xN	$\bar{\nu}$	Total
^{12}C	−2.887E-04		1.833E-02	−7.300E-04			1.732E-02
^{16}O	−1.398E-03		6.793E-03	−1.904E-04	<1.00E-06		5.204E-03
^{27}Al	−1.163E-04		8.665E-04	−2.748E-04	<1.00E-06		4.753E-04
^{56}Fe	−2.432E-03		7.710E-03	−4.424E-03	1.242E-06		8.545E-04
^{52}Cr	−1.571E-03		4.737E-03	−3.999E-03	<1.00E-06		−8.332E-04
^{58}Ni	−2.491E-03		2.924E-03	−5.845E-04	<1.00E-06		−1.511E-04
^{234}U	<1.00E-06	<1.00E-06	<1.00E-06	<1.00E-06	<1.00E-06	1.710E-06	2.039E-06
^{235}U	−5.386E-02	3.735E-01	3.796E-03	−4.125E-03	9.007E-05	5.895E-01	9.089E-01
^{238}U	−2.368E-01	1.096E-01	1.066E-01	−3.446E-02	7.718E-04	1.748E-01	1.206E-01
^{238}Pu	−2.454E-05	1.589E-04	<1.00E-06	−9.902E-07	<1.00E-06	2.295E-04	3.635E-04
^{239}Pu	−1.435E-02	1.477E-01	7.142E-04	−6.188E-04	1.108E-05	2.094E-01	3.429E-01
^{240}Pu	−3.344E-03	8.579E-03	1.821E-04	−2.017E-04	1.778E-06	1.239E-02	1.761E-02
^{241}Pu	−6.644E-04	9.179E-03	2.926E-05	−3.588E-05	2.690E-06	1.294E-02	2.145E-02
^{242}Pu	−1.298E-04	2.530E-04	5.817E-06	−1.000E-05	<1.00E-06	3.646E-04	4.837E-04
^{241}Am	−2.072E-04	1.283E-04	1.236E-06	−3.499E-06	<1.00E-06	1.791E-04	9.793E-05
Total	−3.177E-01	6.492E-01	1.527E-01	−4.966E-02	8.791E-04	1.000E+00	1.435E+00

Table 3
Sensitivity coefficients calculated by Serpent for 3D model with JEFF-3.1.1 - Clean core [pcm/%].

Nuclide	Capture	Fission	Elastic	Inelastic	N,xN	$\bar{\nu}$	Total
^{12}C	−3.327E-04		3.356E-02	−6.867E-04			3.254E-02
^{16}O	−1.356E-03		−1.955E-04	−2.611E-04			−1.813E-03
^{27}Al	−1.128E-04		4.520E-04	−2.970E-04	<1.00E-06		4.217E-05
^{56}Fe	−2.165E-03		6.786E-03	−4.263E-03	<1.00E-06		3.584E-04
^{52}Cr	−1.417E-03		4.895E-03	−3.688E-03	<1.00E-06		−2.098E-04
^{58}Ni	−2.373E-03		2.502E-03	−5.483E-04	<1.00E-06		−4.191E-04
^{234}U	<1.00E-06	1.678E-06	<1.00E-06	<1.00E-06	0.000E+00	2.097E-06	3.775E-06
^{235}U	−5.743E-02	3.781E-01	4.444E-03	−2.671E-03	1.282E-04	6.112E-01	9.338E-01
^{238}U	−2.147E-01	1.018E-01	8.805E-02	−3.156E-02	5.685E-04	1.634E-01	1.076E-01
^{238}Pu	−2.331E-05	1.448E-04	−1.388E-06	<1.00E-06	<1.00E-06	2.118E-04	3.318E-04
^{239}Pu	−1.327E-02	1.423E-01	2.707E-04	−7.398E-04	7.700E-06	2.005E-01	3.291E-01
^{240}Pu	−3.091E-03	8.238E-03	2.375E-04	−1.824E-04	2.225E-06	1.188E-02	1.709E-02
^{241}Pu	−6.156E-04	8.768E-03	5.866E-05	−4.332E-05	2.579E-06	1.231E-02	2.048E-02
^{242}Pu	−1.227E-04	2.357E-04	1.962E-05	−9.358E-06	<1.00E-06	3.379E-04	4.611E-04
^{241}Am	−1.911E-04	1.160E-04	−1.464E-05	−6.897E-06	<1.00E-06	1.642E-04	6.764E-05
Total	−2.972E-01	6.397E-01	1.411E-01	−4.496E-02	7.092E-04	1.000E+00	1.439E+00

clear core is shown in Fig. 15, which indicates that the main contributions to the total uncertainties would be made in the energy range between approximately 1 KeV and 1 MeV, which is the region with the high uncertainties values.

4.2. Axial fuel movements

There are numerous experiments in the SNAEK-12B program. Therefore, presenting all the sensitivity profiles would be exhaustively long and will not provide any meaningful information, especially due to the fact that the two codes (Serpent and ERANOS) are in a good agreement (as shown previously). This section summarizes the propagated uncertainties results for axial fuel movements, as described in Table 1.

The results show that there is a difference in the propagated uncertainties between Serpent and ERANOS. This could be attributed to the codes calculated sensitivity profiles due to geometry variation. The results indicate that Serpent calculations (continuous-energy three-dimensional model) are much more sensitive to variation in the core geometry. Furthermore, as shown in Table 7, the magnitude of the total propagated uncertainties remains low for all the different configurations (below 1 cent). However, in the case of small reactivity changes

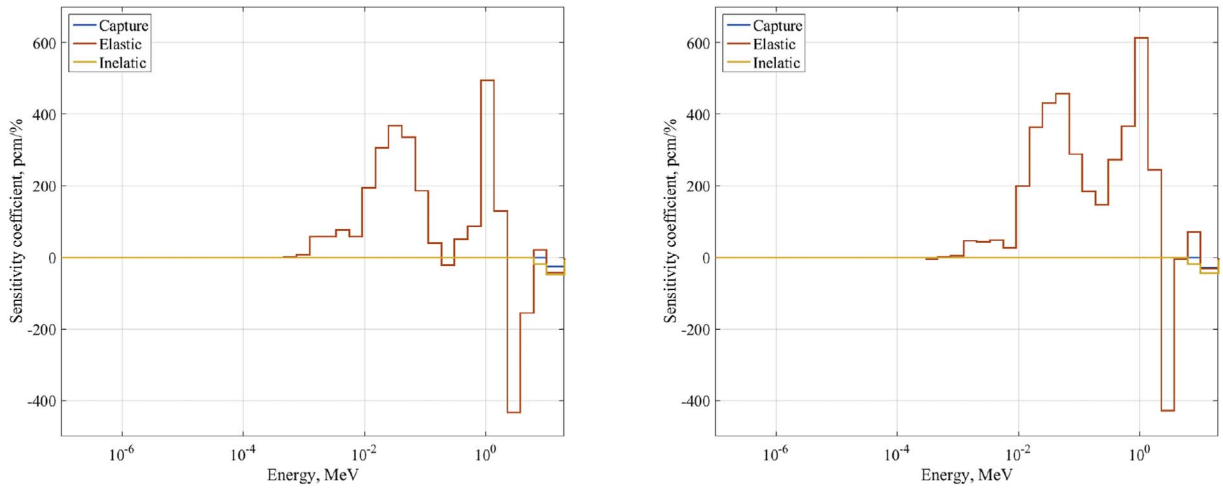

(a) ERANOS.   (b) Serpent.

Fig. 10. Clear criticality core multiplication factor sensitivity to ^{12}C cross-sections.

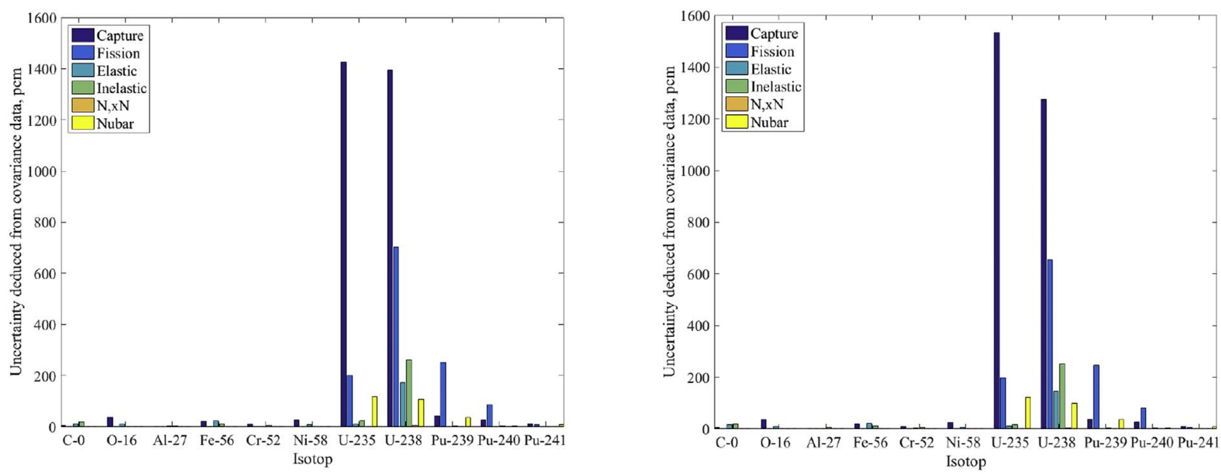

(a) ERANOS.   (b) Serpent.

Fig. 11. Propagated uncertainties for the clear core configuration.

Table 4
Summary of total uncertainty values for the SNEAK-12B clear core configuration [pcm].

	Serpent-COMAC	ERANOS-COMAC
Correlated reactions only	2149	2172
Cross-correlated reaction included	1993	1988

(e.g., experiments 1,2,7,8,9,11,13,22 in Table 7) the total propagated uncertainty could reach (and for some cases exceed) the value of the $\Delta\rho$, as can be seen in Fig. 16, where the error bars represent the total propagated uncertainties calculated by ERANOS and Serpent. The discrepancies between the experimental results and the results obtained from Serpent calculation, for small reactivity variation, could be explained by the associated uncertainties in the nuclear data for almost all the cases. However, the same could not be said regarding the results obtained from ERANOS, which could be attributed, as previously stated, to the limited ability to predict correctly the impact of small geometry perturbation on the sensitivity profiles.

The second set of axial fuel movements consists of experiments with large reactivity variation (more than 1 cent, e.g., experiments -3,4,5,6,10,12,14,15,20,21,23 in Table 7). The total propagated uncertainties remain small, as shown in Fig. 17. The calculated results for large reactivity variation are in good agreement with the experimental data for almost all the cases. Therefore, the main uncertainties in those experiments could be attributed to uncertainties linked to computational schemes (R–Z geometry model and cell calculations in ERANOS, and statistical uncertainties in Serpent).

4.3. Radial fuel movements

The results for the radial material relocation (see Fig. 5) are summarized in this section. The total propagated uncertainties are summarized in Table 8. The results show that the difference between the experimental results and the results calculated by Serpent remains small, but the results calculated by ERANOS increasingly deviate as the number of affected elements increases. On the other hand, the results of the propagated uncertainties are in good agreement between the two codes. This could be attributed to the fact that the radial movement is made along a very flat flux distribution.

Table 5
Summary of uncertainties per reaction for each isotope in SNEAK-12B clear core configuration calculated in ERANOS [pcm].

	Capture	Fission	Elastic	Inelastic	N,xN	NU
^{12}C	5.146E+00		1.121E+01	1.920E+01		
^{16}O	3.781E+01		1.019E+01	1.262E+00	<1.00	
^{27}Al	1.349E+00		2.229E+00	4.291E+00	<1.00	
^{56}Fe	2.030E+01		2.243E+01	1.188E+01	<1.00	
^{52}Cr	9.427E+00		2.100E+00	5.228E+00	<1.00	
^{58}Ni	2.616E+01		7.282E+00	1.206E+00	<1.00	
^{234}U	<1.00	<1.00	<1.00	<1.00	<1.00	<1.00
^{235}U	1.427E+03	2.011E+02	9.406E+00	2.398E+01	<1.00	1.188E+02
^{238}U	1.395E+03	7.024E+02	1.732E+02	2.605E+02	4.363E+00	1.062E+02
^{238}Pu	<1.00	<1.00	<1.00	<1.00	<1.00	<1.00
^{239}Pu	4.147E+01	2.531E+02	1.022E+00	2.481E+00	<1.00	3.626E+01
^{240}Pu	2.787E+01	8.448E+01	<1.00	2.764E+00	<1.00	2.531E+00
^{241}Pu	1.087E+01	6.602E+00	<1.00	<1.00	<1.00	6.994E+00
^{242}Pu	<1.00	<1.00	<1.00	<1.00	<1.00	<1.00
^{241}Am	<1.00	<1.00	<1.00	<1.00	<1.00	<1.00

Table 6
Summary of uncertainties per reaction for each isotope in SNEAK-12B clear core configuration calculated in Serpent [pcm].

	Capture	Fission	Elastic	Inelastic	N,xN	NU
^{12}C	5.995E+00		1.682E+01	1.819E+01		
^{16}O	3.666E+01		9.200E+00	1.756E+00		
^{28}Al	1.301E+00		1.963E+00	4.652E+00	<1.00	
^{56}Fe	1.823E+01		1.967E+01	1.162E+01	<1.00	
^{52}Cr	9.352E+00		2.323E+00	4.831E+00	<1.00	
^{58}Ni	2.504E+01		5.334E+00	1.154E+00	<1.00	
^{234}U	<1.00	<1.00	<1.00	<1.00		<1.00
^{235}U	1.531E+03	1.982E+02	1.145E+01	1.631E+01	<1.00	1.231E+02
^{238}U	1.273E+03	6.544E+02	1.463E+02	2.522E+02	3.168E+00	9.921E+01
^{238}Pu	<1.00	<1.00	<1.00	<1.00	<1.00	<1.00
^{239}Pu	3.844E+01	2.447E+02	<1.00	3.005E+00	<1.00	3.481E+01
^{240}Pu	2.612E+01	8.138E+01	<1.00	2.490E+00	<1.00	2.429E+00
^{241}Pu	1.025E+01	6.318E+00	<1.00	<1.00	<1.00	6.655E+00
^{242}Pu	<1.00	<1.00	<1.00	<1.00	<1.00	<1.00
^{241}Am	<1.00	<1.00	<1.00	<1.00	<1.00	<1.00

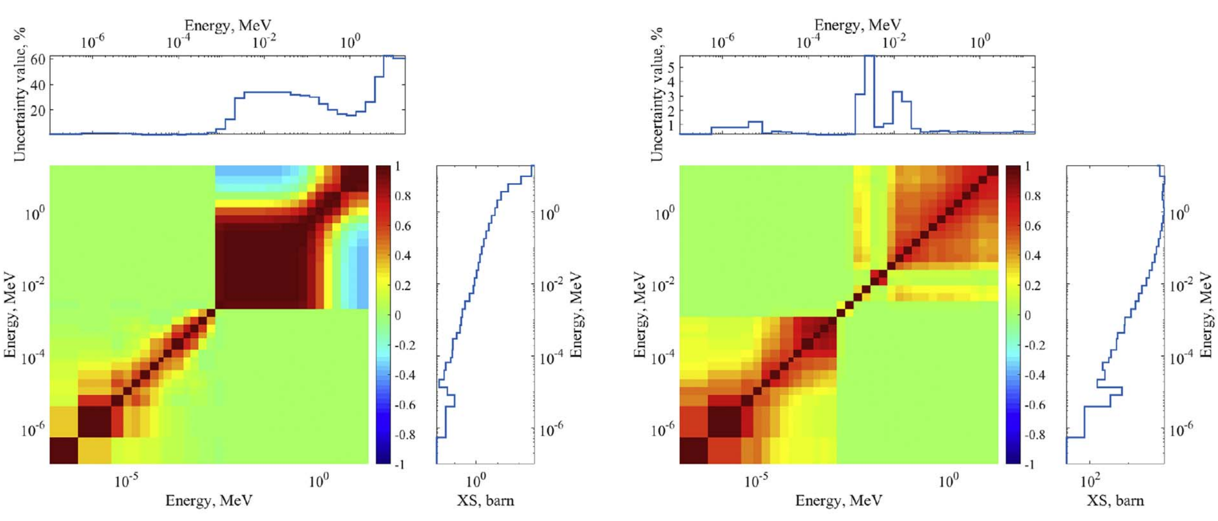

(a) Capture. (b) Fission.

Fig. 12. Covariance data for ^{235}U from COMAC.

4.4. Steel blockage

The different steel blockage geometries are summarized in Table 1 (experiments - 15,16,17,18). Unlike the different experiments in the SNEAK-12A experimental campaign, the densities of the different isotopes were not modified in the SNEAK-12B experimental campaign. This is true except for the steel blockage experiments, which are discussed below.

The data regarding the utilized steel was not found in the available data about the SNEAK-12B experiments. Therefore, it was assumed that the utilized steel was SS-304, which resulted in large differences in the reactivity changes. The results are summarized in Table 9. As in

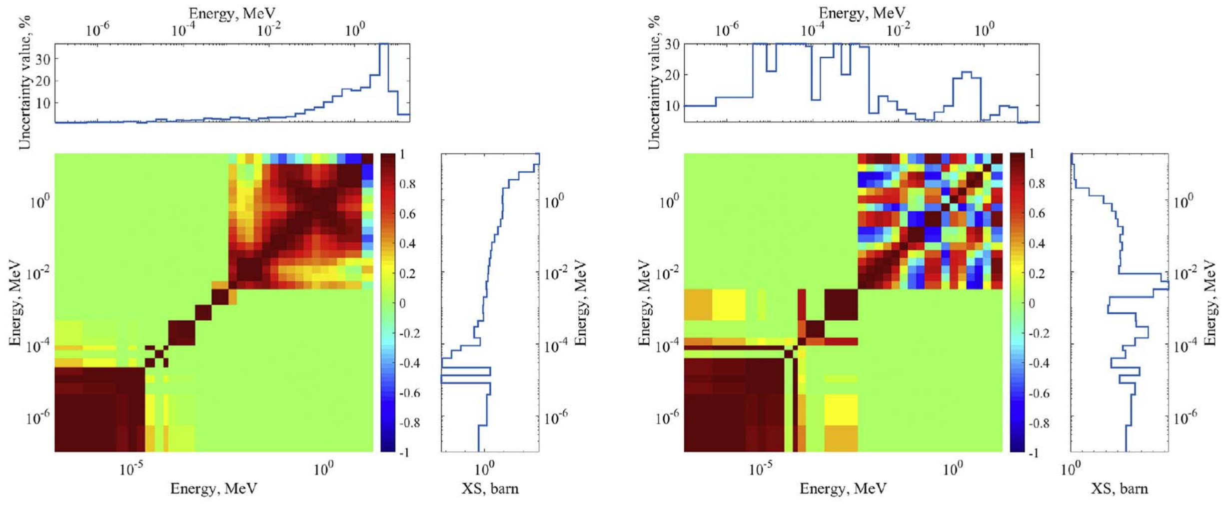

(a) Capture.
(b) Fission.

Fig. 13. Covariance data for ^{238}U from COMAC.

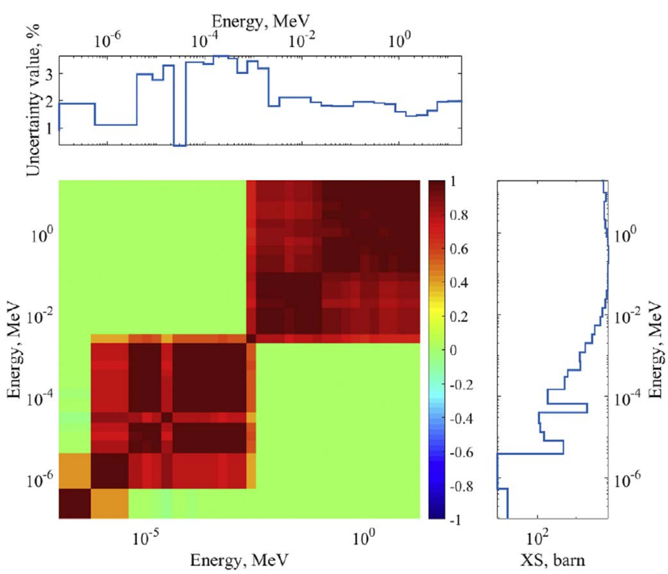

Fig. 14. Covariance data for ^{239}Pu from COMAC.

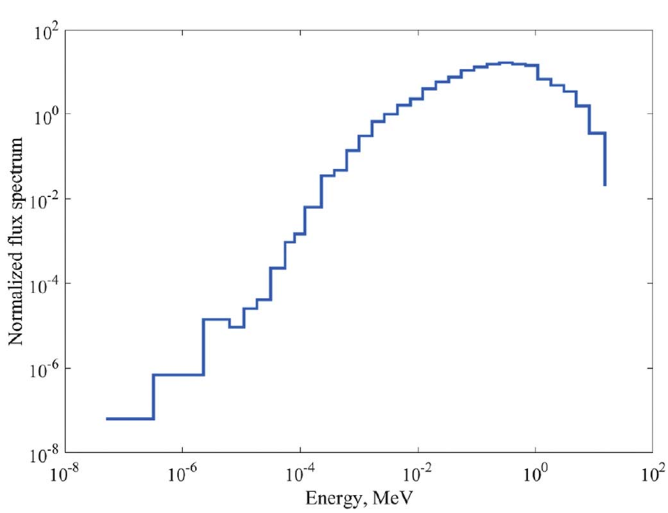

Fig. 15. 33 energy group homogenized flux spectrum for the clear core configuration.

Table 7
Axial fuel redistribution results.

Exp. ID	$\Delta\rho$ [cent]			Total uncertainty [cent]	
	Experimetal	Serpent	ERANOS	Serpent	ERANOS
1	0.15	0.62 ± 0.47	0.29	2.41E-01	2.37E-02
2	0.80	1.08 ± 0.47	0.14	1.79E-01	1.44E-01
3	−1.40	− 1.70 ± 0.47	−1.21	1.01E-01	5.13E-02
4	−5.60	− 4.96 ± 0.47	−6.99	5.37E-02	3.00E-02
5	−2.80	− 1.86 ± 0.47	−2.49	1.43E-01	3.47E-02
6	−10.20	− 9.14 ± 0.47	−9.12	3.59E-02	2.98E-02
7	0.20	0.15 ± 0.47	0.48	1.04E-01	2.12E-02
8	0.80	0.46 ± 0.47	2.48	4.29E-01	2.11E-02
9	0.60	0.31 ± 0.47	0.47	7.56E-01	6.59E-02
10	3.00	2.48 ± 0.47	3.36	1.09E-01	3.66E-02
11	0.50	1.08 ± 0.47	−1.21	2.16E-01	3.23E-02
12	3.85	3.25 ± 0.47	−0.89	1.02E-01	2.15E-01
13	−0.60	− 0.62 ± 0.47	−0.84	3.53E-01	1.21E-02
14	−1.10	− 1.39 ± 0.47	−2.84	1.36E-01	6.61E-03
15	−2.65	− 3.87 ± 0.47	−2.06	2.73E-01	1.26E-02
20	−8.40	− 7.90 ± 0.47	−6.28	3.72E-02	3.76E-02
21	−15.60	− 14.41 ± 0.47	−13.93	2.66E-02	3.21E-02
22	−0.20	− 1.08 ± 0.47	−5.53	2.76E-01	2.51E-02
23	−15.80	− 16.77 ± 0.47	−18.21	1.22E-02	1.24E-02

previous sections, the total propagated uncertainty remains small in comparison to the total reactivity change. Obviously, the actual steel used in the SNEAK-12B experiments was not SS-304. However, it is reasonable to assume that the propagated uncertainties would not change dramatically either qualitatively or quantitatively.

5. Conclusions

A complete sensitivity analysis and uncertainty propagation are performed on the different configuration of the SNEAK-12B experimental program. The assessment of these nuclear data uncertainties is of high importance for future experiments design, which aims to improve the available knowledge of SCA situations and to increase the accuracy of the available nuclear data, as a way to accurately predict reactivity variations inside the core. The calculations of the sensitivity coefficients are carried out by ERANOS, a well-established code for fast reactors, and the newly available capabilities of Serpent 2. All the calculations are base on the JEFF-3.1.1 evaluation.

The sensitivity analysis on the clear core configuration show an excellent agreement between ERANOS and Serpent, with no significant

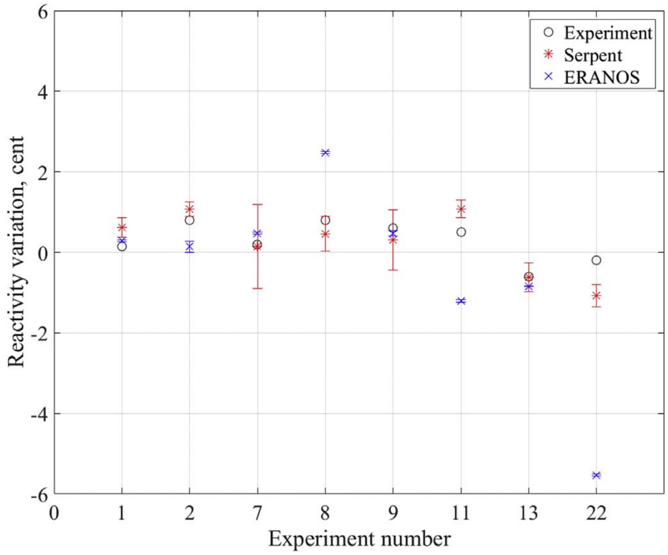

Fig. 16. Propagated uncertainties for configuration with small reactivity changes (less than 1 cent).

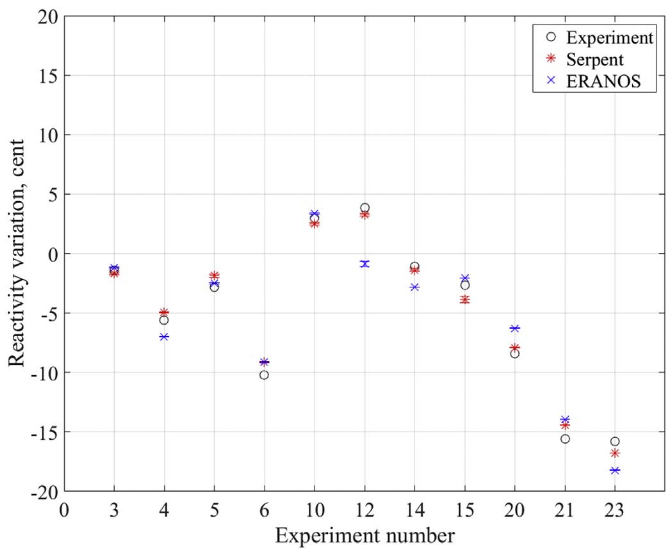

Fig. 17. Propagated uncertainties for configuration with large reactivity changes (greater than 1 cent).

Table 8
Radial fuel redistribution results.

Exp. ID	$\Delta\rho$ [cent]			Total uncertainty [cent]	
	Experimetal	Serpent	ERANOS	Serpent	ERANOS
24	−4.90	−4.80	3.01	5.55E-02	3.19E-02
25	−12.00	−11.78	−8.29	3.24E-02	2.16E-02
26	−14.70	−15.65	−16.80	1.49E-02	1.50E-02
27	−19.10	−19.24	−27.60	1.17E-02	1.30E-02
28	−1.60	−1.39	−0.43	1.38E-01	1.05E-01

deviations (see Figs. 6–10). The small differences could be attributed to the slight difference in material balance and the geometry changes due to the R-Z simplification in ERANOS.

The uncertainty analysis of the clear core experiment, based on the COMAC covariance data, show a large propagated uncertainty value of approximately 2000 pcm (Fig. 11b and a), with the main contributors being the capture cross-sections in the uranium isotopes. This value is

Table 9
Steel blockage results.

Exp. ID	$\Delta\rho$ [cent]			Total uncertainty [cent]	
	Experimetal	Serpent	ERANOS	Serpent	ERANOS
16	0.7	2.17	2.35	8.35E-02	1.90E-02
17	0.9	3.25	2.48	6.68E-02	1.51E-02
18	−8.3	−10.07	−12.76	2.04E-02	6.57E-03
19	1.1	2.17	3.06	8.73E-02	1.74E-02

slightly lower in comparison to SNEAK-12A clear core, which had a total propagated uncertainty values of about 2500 pcm, remains quite high in comparison to other typical fast latices (sodium and liquid metal fast reactors), e.g., the ASTRID-like core total propagated uncertainties make about 1300 pcm on the core effective multiplication factor (Garcia-Herranz et al., 2016). Although the test zone was loaded with MOX fuel, a large amount of enriched uranium in the periphery is the main reason for the high level of uncertainty.

The values of propagated uncertainties on reactivity variation between the different configurations are also evaluated. The results (Tables 7–9) show that for small reactivity variations the propagated uncertainties are quite high with respect to the reactivity change magnitude, as shown in Fig. 16. On the other hand, for large reactivity changes, the propagated uncertainties remain small, as shown in Fig. 17. This is the result of large nuclear data uncertainties for some of the isotopes, which are magnified in light of the small reactivity changes. The results also show that there is a difference between ERANOS and Serpent in terms of uncertainty values calculations. As demonstrated for small reactivity changes in Fig. 16, ERANOS underestimates the reactivity variation for some of the configuration, and this propagates into the sensitivity calculations.

This work conclude the current re-evaluation of the SNEAK-12A and 12B experimental programs. The results of this work highlight the fact that there are (still) large uncertainty values associated with several of the investigated isotopes cross-section, mainly capture in the uranium isotopes. A preliminary study on the impact of the examined experiments on the nuclear data is made. This study reveals that for the examined experiments the JEFF-3.1.1 evaluation is sufficient for accurate core behavior prediction. The SNEAK-12 series of experiments is proved to be an excellent benchmark for improving nuclear data knowledge, mainly for uncertainties reduction in case of SCA situation. This benchmark enables better prediction of reactivity effects and lay the foundations for future experiments design of similar programs in the ZEPHYR facility.

Acknowledgment

The research was partially funded by the Israeli ministry of National Infrastructures, Energy, and Water Resources under contract number 215-11-020.

References

Aufiero, M., Palmiotti, G., Salvatores, M., Sen, S., 2016. Coupled reactors analysis: new needs and advances using Monte Carlo methodology. Ann. Nucl. Energy 98, 218–225. http://www.sciencedirect.com/science/article/pii/S0306454916302584 https://doi.org/10.1016/j.anucene.2016.08.002.

Aufiero Maand Bidaud, A., Hursin, M., Leppanen, J., Palmiotti, G., Pelloni, S., Rubiolo, P., 2015. A collision history-based approach to sensitivity/pertubation calculations in the continues energy Monte Carlo code Serpent. Ann. Nucl. Energy 85, 245–258.

Bertrand, F., Marie, N., Prulhire, G., Lecerf, J., Seiler, J., 2016. Comparison of the behaviour of two core designs for ASTRID in case of severe accidents. Nucl. Eng. Des. 297, 327–342. http://www.sciencedirect.com/science/article/pii/S0029549315001478 https://doi.org/10.1016/j.nucengdes.2015.04.020.

Blaise, P., Boussard, F., Ros, P., Leconte, P., Margulis, M., Martin, G., Blandin, K., 2016. Advanced small and large core distortion modeling in ZPR to assess core recriticality scenarios of SFR core degradation sequences. In: Proc. Int. Conf. IGORR-2016. European Nuclear Society, Berlin Germany.

De Saint Jean, C., Archier, P., Noguere, G., Litaize, O., Vagli-Gaurard, C., Bernard, D., Leray, O., 2012. Estimation of multi-group cross sections covarinaces. In: Proc. Int. Conf. PHYSOR-2012. American Nuclear Society, Knoxville,TEN,USA.
Frohlich, R., Helm, F., Kessler, G., Kiefhaber, E., 1980. Safety Related Physics Activitites in the DEBENE-FBR-Project. Tech. Rep. KfK 3082. pp. 1–28.
Gabrielli, F., Rineiski, A., Vezzoni, B., Maschek, W., Fazio, C., Salvatores, M., 2015. Astrid-like fast reactor cores for burning plutonium and minor actinides. Energy Procedia 71, 130–139. http://www.sciencedirect.com/science/article/pii/S1876610214026927 https://doi.org/10.1016/j.egypro.2014.11.863 the Fourth International Symposium on Innovative Nuclear Energy Systems, INES-4.
Garcia-Herranz, N., Panadero, A.L., Matrinez-Campo, A., Pelloni, S., Mikityuk, K., Pautz, A., 2016. Nuclear data sensitivity and uncertainty assessment of sodium voiding reactivity coefficients of an ASTRID-like Sodium Fast Reactor. In: Proc. Int. Conf. On Nuclear Data for Science and Technology, pp. 1–9.
Ivanov, E., Duranti, A., 2006. SNEAK 7A and 7B Pu-fueled fast critical assemblies in the Karlsruhe fast critical facility. In: International Handbook of Evaluated Reactor Physics Benchmark Experiments (IRPhE), NEA/NSC/DOC(2006)1, March 2015 Edition.
Ivanov, E., Ivanova, T., Pignet, S., 2013. Sensitivity and uncertainty analyses aplplied to neutronics calcualtions for safety assessment at IRSN. In: Proc. of the Int. Conf. on Fast Reactors and Related Fuel Cycle: Safe Technology and Sustainable Scenarios (FR13). IAEA, Paris, France.
Leppanen, J., Pusa, M., Viitanen, T., Valtavirta, V., Kaltiaisenaho, T., 2015. The Serpent Monte Carlo code: status, development and applications in 2013. Ann. Nucl. Energy 82, 142–150.
Margulis, M., Blaise, P., Mellier, F., Gilad, E., 2017a. The path for innovative severe accident neutronics studies in ZPRs. Part I.2-Impact of nuclear data uncertainties on reactivity changes of SNEAK-12A core. Prog. Nucl. Energy 96, 97–117.
Margulis, M., Blaise, P., Gabrielli, F., Gruel, A., Mellier, F., Gilad, E., 2017b. The Path for Innovative Severe Accident Neutronics Studies in ZPRs. Part II.1-Analysis of SNEAK-12B Experiments for Core Disruption in LMFBRs. Manuscript subitted for publication. .
Margulis, M., Blaise, P., Gabrielli, F., Gruel, A., Mellier, F., Gilad, E., 2017c. The path for innovative severe accident neutronics studies in ZPRs. Part I.1-Analysis of SNEAK-12A experiments for core disruption in LMFBRs. Prog. Nucl. Energy 94, 106–125. https://doi.org/10.1016/j.pnucene.2016.12.006.
Margulis, M., Blaise, P., Buiron, L., Pruhliere, G., Fontaine, B., Gilad, E., 2017d. Representativity studies of ZEPHYR fast/thermal coupled core for SFR-like reactivity effects during core meltdown. In: Proc. of ICAPP 2017. Fukui/Kyoto, Japan, pp. 1–8.
Margulis, M., Blaise, P., Buiron, L., Gilad, E., 2017e. ZPR core representativity of SFR reactivity effects during core meltdown. In: Trans. American Nuclear Society; Vol. 117. Washingto DC, USApp. 1503–1506.
Ohshima, H., Kubo, S., 2016. Sodium-cooled fast reactor. In: Pioro, I.L. (Ed.), Handbook of Generation IV Nuclear Reactors; Chap. 5. Woodhead Publishing Series in Energy. Woodhead Publishing, 978-0-08-100149-3, pp. 97–118. https://www.sciencedirect.com/science/article/pii/B9780081001493000057 https://doi.org/10.1016/B978-0-08-100149-3.00005-7.
Ros, P., Leconte, P., Blaise, P., de Spville, H.D., Maillot, M., 2017. Fast-thermal coupled cores in zero power reactors: a demonstration of feasibility and pertinence for the ZEPHYR project. Ann. Nucl. Energy 290–305. http://www.sciencedirect.com/science/article/pii/S0306454917301640 https://doi.org/10.1016/j.anucene.2017.06.019.
Ruggieri, J.M., Tommasi Jamd Lebart, J.F., Suteau, C., Plisson-Rieunier, D., De Saint Jean, C., Rimpault, G., Sublet, J.C., 1973. ERANOS 2.1: international code system for GEN IV fast reactor analysis. In: Proc. ICAAP2006. American Nuclear Society, Reno, NV, USA.
Rullhusen, P., April 2005. Nuclear Data Needs for Generation IV Nuclear Energy Systems.
Salvatores, M., Jacqmin, R., Aliberti, G., Dunn, M., Hogenbrik, A., Ignatyuk, A., Ishikawa, M., Kodeli, I., Koning, A., McKnight, R., Mills, R.W., Oblozinsky, P., Palmioti, G., Plompen, A., Rimpault, G., Rugama, Y., Talou, P., Yang, W.S., January 2008. Uncertainty and target accuracy assessment for innovative systems using recent covariance data evaluation. Tech. Rep. NEA/WPEC-26, International Evaluation Cooperation. vol. 26 OECD Nuclear Energy Agency978-92-64-99053-1.
Tommasi, J., Archier, P., Rimpault, G., 2010. Sodium void validation with ERANOS on zero power facility experiments. In: Proc. PHYSOR-2010. American Nuclear Society, Pittsburg,PA,USA.